

## Optically induced second-harmonic generation in CdI<sub>2</sub>-Cu layered nanocrystals

This article has been downloaded from IOPscience. Please scroll down to see the full text article.

2003 J. Phys.: Condens. Matter 15 2309

(<http://iopscience.iop.org/0953-8984/15/14/306>)

View [the table of contents for this issue](#), or go to the [journal homepage](#) for more

Download details:

IP Address: 171.66.16.119

The article was downloaded on 19/05/2010 at 08:38

Please note that [terms and conditions apply](#).

# Optically induced second-harmonic generation in CdI<sub>2</sub>–Cu layered nanocrystals

F Voolless<sup>1</sup>, H Korme<sup>1</sup> and W Hydaradjan<sup>2</sup>

<sup>1</sup> Chemical and Electrophysical Department, Stockholm Technological University, Kunglika Tekniska Högskola, Sweden

<sup>2</sup> Stockholm University, Chemical Division, SE-10044, Sweden

E-mail: avoolless@hotmail.com

Received 3 December 2002, in final form 7 March 2003

Published 31 March 2003

Online at [stacks.iop.org/JPhysCM/15/2309](http://stacks.iop.org/JPhysCM/15/2309)

## Abstract

A large enhancement (up to 0.40 pm V<sup>-1</sup>) of the second-order optical susceptibility was observed in CdI<sub>2</sub>–Cu single-layered nanocrystals for the Nd:YAG fundamental laser beam  $\lambda = 1.06 \mu\text{m}$ . The Cu impurity content and nanolayer thickness of the cleaved layers (about several nanometres) play a crucial role in the observed effect. The temperature dependence of the optical second-harmonic generation (SHG) together with its correlation with Raman spectra of low-frequency modes indicate a key role for the UV-induced anharmonic electron–phonon interactions in the observed effect. The maximal output UV-induced SHG was achieved for a Cu content of about 0.5% and at liquid helium temperatures.

(Some figures in this article are in colour only in the electronic version)

## 1. Introduction

CdI<sub>2</sub> layered single crystals (space group C<sub>6v</sub><sup>4</sup>) possess an intermediate structure between wide-bandgap alkali halide crystals (energy gap about 3.75 eV at room temperature) and molecular crystals [1]. They have a large anisotropy of chemical bonds [2]. Significant intralayer ionic–covalent chemical bonds and weak interlayer van der Waals bonds raise the possibility of their use in devices similar to heterojunctions in semiconducting microelectronics. This anisotropy may also make it possible to obtain very thin layers (up to several nanometres, possessing striking optical quantum size-confined effects due to presence of the thin nanolayers) using the usual method of cleavage by glue tape [3]. This anisotropy may be used during the search for new nonlinear optical materials requiring large charge density non-centrosymmetry [4]. Band structure calculations for CdI<sub>2</sub> have shown [5–8] a large anisotropy in the space charge density distribution determining the anisotropy in the corresponding optical spectra. In [9, 10] the observation of second-order optical effects in non-centrosymmetric polytypes of CdI<sub>2</sub>

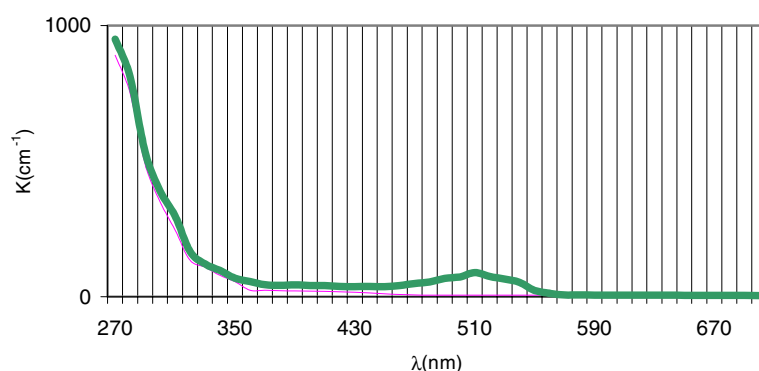


**Figure 1.** Typical room-temperature absorption spectra of the pure  $\text{CdI}_2$  (thin curve) and  $\text{CdI}_2$ -Cu (0.8% in weight units) (thick curve) nanolayers at a thickness of about 2 nm.

was reported. The value of the output second-order optical susceptibility was low. One promising way to enhance the corresponding nonlinear optical susceptibilities consists of using semiconducting nanocrystals [11, 12] and of photoinduction by nonlinear optical methods [13]. Another way to increase the local second-order optical constants consists of the appropriate doping of  $\text{CdI}_2$ . Kityk *et al* [14] have shown that doping with Cu leads to giant charge density non-centrosymmetry that may even favour appearance of pyroelectricity and ferroelectricity.

The origin of the increase in local different optical constants may be related to electron-phonon anharmonicity. However, one cannot fully exclude the role played by photostimulated 'copper defect' complexes with low activation energy [15]. The latter are also light sensitive.

In the present paper we report investigations into photoinduced second-harmonic generation (SHG) in  $\text{CdI}_2$  layered nanocrystallites (with thicknesses of 1–6 nm) doped with Cu. Such thicknesses usually cause additional contributions from size-confined effects, favouring enhanced second-order optical susceptibilities [11, 14].

We will present experimental investigations of the photoinduced SHG versus thickness of the  $\text{CdI}_2$  layers and their concentration at different temperatures. It was shown earlier [16, 17] that there is the possibility of enhancement of second-order optical constants during cooling.

## 2. Experimental details

The Bridgman–Stockbarger method was used for crystal growth from a mixture of the pure  $\text{CdI}_2$  and CuI re-refined materials taken in the appropriate ratio. The cuprous concentration in the batch was 0.08–1%. Control of the  $\text{CdI}_2$  structure was verified using an x-ray diffractometer. An optical polarimeter was used to control the homogeneity of the sample. We found that the non-uniformity of the samples was about the  $10^{-3}\%$ . The cleaved samples had sizes of about  $4 \times 8 \text{ mm}^2$  and the sample thickness was controlled using an rf interferometer as described in [3]. Typical absorption spectra of pure and Cu-doped samples are presented in figure 1. One can see a slight shift of the absorption edge towards higher wavelengths as well as occurrence of a slight absorption at about 480–540 nm. The effective energy gap (about 3.75 eV) is in agreement with the value obtained in [3, 5–9].

The photoinduced SHG was measured using a method similar to that described in [18] (see figure 2). As the pumping UV laser we used a pulsed excimer  $\text{XeF}^*$  laser with a pulse time duration of about 40 ps, a power of about 35 MW/pulse and a wavelength of about 371 nm.

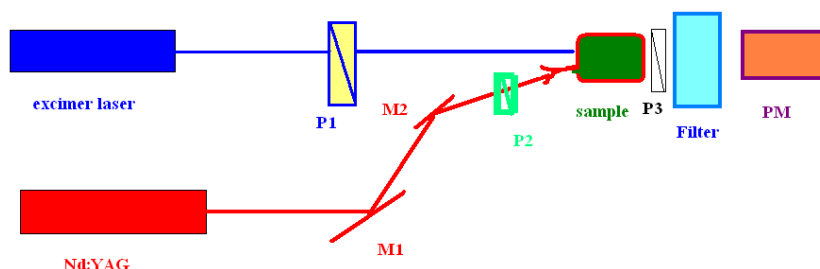


Figure 2. Experimental set-up for the measurement of the photoinduced SHG.

Its beam profile sequence was roughly 3–4.5 mm in diameter. As a fundamental laser for the SHG we used an Nd–YAG laser (with  $\lambda = 1.06 \mu\text{m}$ , pulse duration about 25 ps and power 17 MW /pulse). The pulse frequency repetition was about 0.1 Hz. Separation of the frequency-doubled green signal ( $\lambda = 0.53 \mu\text{m}$ ) from the input fundamental 1.06  $\mu\text{m}$  signal was achieved by the use of a green interferometer filter and grating monochromator with a resolution of about  $7 \text{ nm mm}^{-1}$ . A photomultiplier with a relaxation time resolution of about 1 ns was used for detection of the doubled-frequency output green SHG signal. An electronic boxcar integrator with a gate equal about 650 ps was used for registration of the output SHG. To eliminate the luminescence we measured the output angle-dependent background using a sphere-like quantameter; this showed that under illumination of the UV laser the maximal output SHG was observed for  $\lambda = 475 \text{ nm}$  and was absent in the region of 553 nm. Independently we found that the decay times of the SHG, several picoseconds, was three orders less than that of the corresponding luminescent signals.

The geometry of the performed experiment satisfied quasi-phase-matched conditions, which in this case required an angle of  $31.5^\circ$  between the  $Z$  and  $Y$  axes of the single-axis CdI<sub>2</sub> crystals. The detection was performed for light polarization corresponding to the  $d_{14}$  tensor components.

### 3. Results and discussions

Without the UV pump excimer laser illumination the SHG output signal possessed an intensity of about  $10^{-5}$  with respect to the incident fundamental ones. After the UV treatment the output signal was at least one order higher and was equal to about  $10^{-3}$ – $10^{-4}$  compared with the fundamental ones. At lower temperatures (particularly below 80 K) the output photoinduced SHG signal increased considerably.

Figure 3 shows the measured dependence of the output SHG for the CdI<sub>2</sub>-Cu samples (for thickness  $d = 1.6 \text{ nm}$ ) on excimer laser pump power density. For the 40 ps excimer laser pulses one can see a strong increase in the output SHG for all the samples at photoinducing power densities up to  $80 \text{ MW cm}^{-2}$ . Afterwards the SHG dependences appear to be saturated. In the saturation power range (higher than  $85 \text{ MW cm}^{-2}$ ) the intensity of the output SHG for a Cu content of 0.5% (in weight units) seems to be at least three times larger than for a Cu concentration of 0.1%. With the next increase in Cu content up to 0.9% the output SHG begins to decrease and is only a little higher than for the Cu content of 0.1% (see figure 3). Microstructural x-ray analysis shows that the observed decrease is correlated with the creation of Cu agglomerates, which substantially suppress the second-order susceptibilities directly connected with the output photoinduced SHG. So one can say that there is an optimal Cu concentration corresponding to the maximal output SHG signal. The measurements were

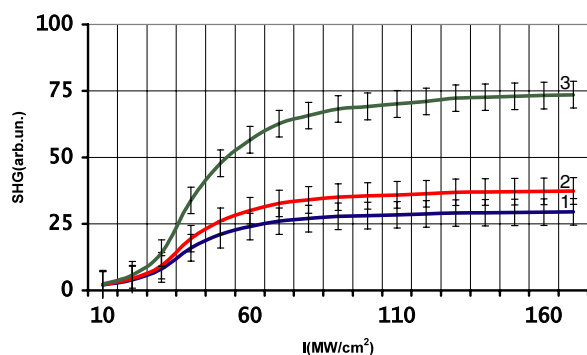


**Figure 3.** Pump power dependences of the photoinduced SHG for the samples possessing different Cu content: curve 1—0.1%; curve 2—0.9%; curve 3—0.5% at  $T = 77$  K and thickness  $d = 1.6$  nm.

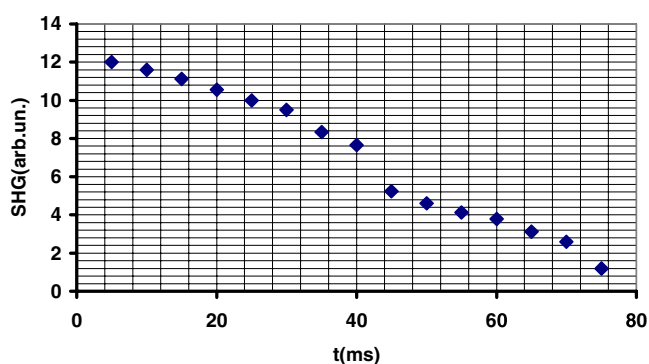


**Figure 4.** Typical dependence of the output SHG signal versus different delay times between the pumping photoinduced 371 nm excimer laser beam and the fundamental Nd:YAG laser beams (with time duration 40 ps) at  $T = 77$  K. The thickness of the cleaved specimen is 1.6 nm.

done for quasi-matched conditions with slight variation of the incident fundamental laser beam. From the obtained angle dependences of the SHG, values of the tensor components  $d_{14}$  were evaluated. The highest  $d_{14}$  value was about  $0.35 \text{ pm V}^{-1}$ . It is necessary to emphasize that during the evaluations of  $d_{14}$  the absorption of the  $\text{CdI}_2\text{-Cu}$  nanolayers was taken into account.

With the next increase in thickness up to 5 nm the output SHG was strongly diminished. This may be a striking manifestation of the important role played by thin nanolayers. So one can say that the observed effect is unambiguously connected with the thin  $\text{CdI}_2\text{-Cu}$  layers.

This deeper understanding the origin of the observed SHG explains the pump–probe dependence of the SHG. The set-up allowed us to perform measurements of delay times within the range 100 ps–500 ms. The relaxation time of the output SHG was equal to about 42–80 ms (see figure 4). Such times are typical of the relaxation of particular layers [3].

One can observe at least two kinks (at about 40 and 70 ms) in the corresponding SHG pump–power dependences. Interlayer rigid phonons [3] may make a significant contribution in this case.

From the obtained experimental data (see figures 3 and 4) it is clear that the UV-induced SHG exists only in the thin (below 3 nm)  $\text{CdI}_2\text{-Cu}$  nanolayers. It is known [11–13] that the nanostructure may stimulate an additional increase in the second-order nonlinear optical

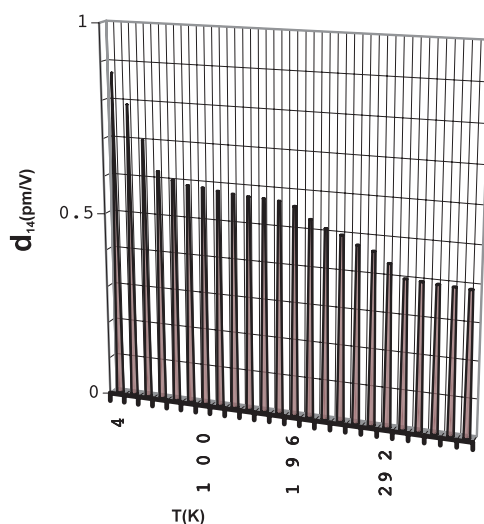


**Figure 5.** Temperature dependence of the second-order  $d_{14}$  tensor component for the fundamental Nd<sup>3+</sup>:YAG laser beam and a photoinduced excimer laser density power of about 40 MW cm<sup>-2</sup> for the samples with a thickness of 1.6 nm.

effects. So the main role of the thin layers is additional enhancement of the second-order optical susceptibilities. This is particularly important for excitonic complexes typical of CdI<sub>2</sub> crystals [19].

For pure crystalline films the output SHG corresponds to the second-order optical susceptibilities  $d_{14}$  equal to about 0.07 pm V<sup>-1</sup>. In [14] the possibility of substantial increase of the output SHG due to doping by the Cu was shown. It was demonstrated that a dominant contribution to the observed second-order optical susceptibility gives enhanced electron-phonon anharmonicity near the cuprous impurity. However, one cannot fully exclude the possibility of another explanation.

The insertion of the Cu ions favours a stronger local electron-phonon interaction, particularly its anharmonic part. The particular role of the local electron-phonon anharmonicity (described by a third-rank polar tensor) is described by third-order rank tensors as in disordered systems [20]. The application of external polarized pumping light aligns the local anharmonic dipole moments [18]. Independent confirmation of this fact may be seen in the relatively large third-order susceptibility of pure CdI<sub>2</sub> crystals [21, 22].

Decrease of the SHG with increasing Cu content may be caused by agglomeration of the Cu impurities that is typical of such types of layered crystals and that has been observed by luminescence [17]. The millisecond relaxation of the photoexcited states may prove the central role of the Cu cluster complexes [14]. Creation of Cu agglomerates favours a reduction in the active electron-phonon centres, effectively contributing to the non-centrosymmetry of the output charge density. The creation of the Cu agglomerates also leads to the occurrence of metallic clusters which additionally scatter light.

The temperature dependence of the SHG shows significant increase of the SHG at low temperature (see figure 5). This increase correlates well with the increasing interlayer anharmonic phonon interactions observed in [5]. So one can expect that the interlayer phonons might play an important role in the observed SHG effects. To verify this prediction we have made additional investigations of UV-induced low-frequency phonon modes originating from interlayer phonon modes by Raman scattering at the wavelength of the Ar laser ( $\lambda = 522$  nm).

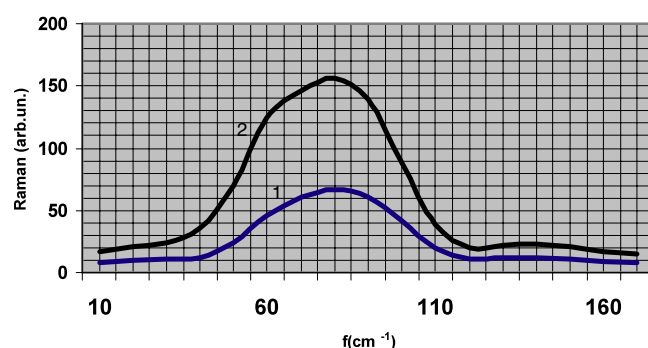


**Figure 6.** Behaviour of the low-frequency phonon modes under of pump excimer laser of different power densities: curve 1—15 MW cm<sup>-2</sup>; curve 2—110 MW cm<sup>-2</sup> at  $T = 77$  K for a sample thickness of 1.6 nm.

One can see (see figure 6) a drastic increase in the low-frequency Raman modes due to UV-induced power treatment, which offers independent confirmation of the contribution of electron–phonon anharmonic mechanisms to the non-centrosymmetry [14, 20]. However, additional investigations of the observed phenomena are now in progress and will be the subject of future publications.

#### 4. Conclusions

Substantial growth of the UV-induced SHG in thin (several nanometres) CdI<sub>2</sub>–Cu nanocrystals (up to 0.40 pm V<sup>-1</sup>) was observed. Maximal output SHG is achieved at a Cu content of about 0.5% in weight units and is limited by the creation of metallic agglomerates at higher Cu concentrations. Moreover, with the next increase in Cu concentration we have a decrease of the output SHG signal due to metallic agglomeration.

The observed effect may be a consequence of additional charge density non-centrosymmetry due to Cu-induced local electron–phonon anharmonic interaction, nanosized quantum confined effects and specific band structure properties of the investigated nanolayers. An increase of the SHG at low temperatures correlates well with enhanced numbers of low-energy phonon interlayer rigid modes effectively contributing to the output SHG. This increase also correlates with the increasing interlayer anharmonic phonon interactions. Additional investigations of low-frequency phonon modes originating from interlayer phonon modes by Raman scattering have shown a drastic increase in low-frequency Raman modes due to UV-induced power treatment which may be an independent confirmation of the electron–phonon anharmonic mechanisms of the non-centrosymmetry [14, 20].

#### References

- [1] Wells A F 1975 *Structural Inorganic Chemistry* (Oxford: Clarendon) p 209
- [2] Kondo S, Mitsunari T and Matsumoto H 1980 *Mem. Fac. Eng. Fukui Univ.* **28** 15
- [3] Kityk I V 1985 *Izv. Vuzov, Ser. Fizika* **28** 102  
Kityk I V 1985 *Zh. Prikl. Spektrosk.* **42** 487
- [4] Zyss J 1974 *Nonlinear Optics* (New York: Academic)
- [5] McCanny J V, Williams R H, Murray R B and Kemény P C 1977 *J. Phys. C: Solid State Phys.* **10** 4255
- [6] Bordas J, Robertson J and Jakobsson A 1978 *J. Phys. C: Solid State Phys.* **11** 2607

- [7] Robertson J 1979 *J. Phys. C: Solid State Phys.* **12** 4753
- [8] Coehoorn R, Sawatzky G A and Haas C 1985 *Phys. Rev. B* **31** 6739
- [9] Nakagawa H, Yamada T, Matsumoto H and Hayashi T 1987 *J. Phys. Soc. Japan* **56** 1185  
Tyagi P, Vedeshwar A G and Mehra N C 2001 *Physica B* **304** 166
- [10] Bolesta I M, Kityk I V and Turchak R M 1994 *Phys. Status Solidi* **36** 892
- [11] Alivisatos A P 1996 *Science* **271** 933
- [12] Norris D J and Bawendi M G 1996 *Phys. Rev. B* **53** 16338
- [13] Varga J, Szingvari Y and Ferenctchi E 2002 *Opt. Laser Technol.* **34** 425
- [14] Kityk I, Pyroha S A, Mydlarz T, Kasperczyk J and Czerwinski M 1998 *Ferroelectrics* **205** 107
- [15] Bondar V 2000 *Mater. Sci. Eng. B* **71** 258
- [16] Bolesta I M, Kityk I V, Filipecki J and Zount H 1995 *Phys. Status Solidi b* **189** 357
- [17] Gloskovska N K, Bieleninik J, Kityk I V, Kasperczyk J, Panasiuk M R and Yaritska L I 1996 *Solid State Commun.* **100** 149
- [18] Kityk I V 2001 *J. Non-Crystalline Solids* **292** 184
- [19] Fukui K, Asakara K, Niimi K, Ishizue I and Nakagawa H 1999 *J. Electron Spectrosc. Relat. Phenom.* **101–103** 299
- [20] Makowska-Janusik M, Kityk I V, Berdowski J, Matejec J, Kasik I and Mefleh A 2000 *J. Opt. A: Pure Appl. Opt.* **2** 43
- [21] Miah M I and Idrish M 2001 *Opt. Mater.* **18** 231
- [22] Sreelatha K, Vengopol C, Chandhary S K and Unnikrishnan N V 1999 *Cryst. Res. Technol.* **34** 897